



## Prediction of low frequency sound fields in buildings near railway lines

Albano Neves e Sousa<sup>a)</sup>

Isabel Lopes<sup>c)</sup>

UTL – Technical University of Lisbon, IST, DECivil, ICIST  
Av. Rovisco Pais, 1, 1049-001 Lisbon, Portugal

Ana Carreira<sup>b)</sup>

UALG – Algarve University, ISE, DEC  
Campus da Penha, 8005-139 Faro, Portugal

**The design of new buildings in the vicinity of railway lines must consider protection against noise and vibrations induced by railway traffic. However, the prediction methods available involve heavy numerical models which have frequency limitations.**

**In this paper a prediction method combining finite elements (FEM) with natural mode analysis is presented for use in reinforced concrete buildings with heavy walls. The method considers 2D FEM models of the railway, ground and buildings to identify the transfer function of vibration from the railway to building foundations. Also 3D models of the buildings are considered to identify the transfer functions of vibration from foundations to walls and floors. Finally, as the impedance of heavy walls and floors is much higher than the acoustic impedance of air, the numerically assessed vibration fields of walls and floors are used to calculate sound fields in rooms by means of natural mode analysis.**

**A set of *in situ* measurements were made in two different situations in order to calibrate the prediction method and also to identify the factors which most affect vibration and sound transmission.**

### 1 INTRODUCTION

This paper reports on the characterisation of the vibration and noise levels expected in multi-storey buildings with multi-level basements for car-parking constructed in the vicinity of underground and surface railway stations. Two cases were studied in Lisbon, Portugal: a) residential building near Saldanha underground metro station; and b) office building near Alvalade surface metro station.

---

<sup>a)</sup> email: albano.nsousa@civil.ist.utl.pt

<sup>b)</sup> email: ascarrei@ualg.pt

<sup>c)</sup> email: ilopes@civil.ist.utl.pt

The study was divided into the following parts: dynamic characterisation of the source, ground, building, and adjacent buildings when existing; and sound field characterisation in the buildings.

## 2 CHARACTERISATION OF THE SOURCE

In order to characterise the vibration induced by the railway traffic on the ground, triaxial acceleration measurements were performed close to the railway lines in the Metro stations near the construction site. As the railway line adjacent to the building in case a) was still on construction when the study was carried out, measurements were performed in an existing Metro station nearby.

Fig. 1 shows the lower and higher envelopes of the one-third octave band measured acceleration spectra, which are in good agreement with published measured spectra<sup>1,2</sup>. An average acceleration spectrum is also shown in case a). In general, the spectra exhibit high energy content in the frequency range 31.5 – 100 Hz. Velocity peaks also were identified at 8 and 10 Hz in case b).

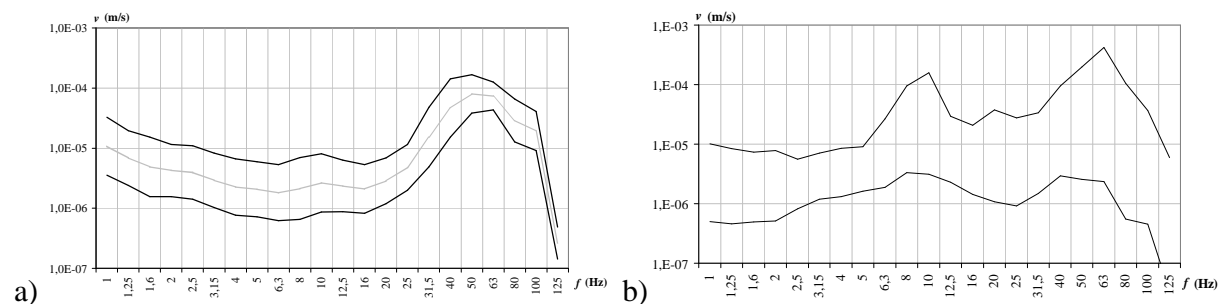


Fig. 1 Envelopes and average of the one-third octave band measured acceleration spectra in cases a) and b).

As the railway line in the existing Metro station considered in case a) is non-isolated, whereas the line in the on-construction station will be installed on a concrete shell separated from the station structure by a resilient mat, which will reduce the natural frequency of the system of about 60 – 70 % and thus the actual vibration of about 10 – 20 %, the lower envelope of the measured acceleration spectra is assumed to provide an acceptable estimate of the vibration at the source. In spite of this assumption, the spectra shown in Fig. 1 were considered in the study to describe ground excitation.

## 3 CHARACTERISATION OF THE ADJACENT EXISTING BUILDINGS

2D FEM models<sup>3</sup> were used to characterise the transmission of vibration from the underground railway station to the building. The model included also the existing adjacent buildings, in case a), and therefore measurements had to be performed in order to assess their dynamic properties. In one of the buildings, with a reinforced concrete frame structure, the measurements indicated natural frequencies of 2.0 and 3.3 Hz associated with the first two translational vibration modes and also a natural frequency of 4.3 Hz associated with a torsional vibration mode. In the other building, with a masonry wall-type structural system, acceleration peaks appeared at 2.6 and 3.7 Hz, but the associated vibration modes were not identified.

## 4 CHARACTERISATION OF THE GROUND

### 4.1 Ground profile

Assessment of the ground profile was based on field test data, mainly SPT (Standard Penetration Test), and other published information<sup>4 to 6</sup>. In case a), the ground profile included 2.0 to 3.0 m superficial backfill, followed by stiff clay with depth increasing strength ( $29 \leq N \leq 60$ ). In case b), the ground profile included 1.6 to 8.0 m superficial backfill and alluvium followed by sand, clay or silt according to the location.

For the small displacements induced by railway traffic, the ground exhibits a linear (elastic) behaviour and therefore ground response is mainly controlled by the shear wave velocity,  $v_S$  (m/s). Empirical equations were used to obtain 3D profiles of the shear wave velocity. Fig. 2 was obtained for cases a) and b) with the equation given by Otha and Goto<sup>7</sup> ( $v_S = 85 N^{0.348}$ ).

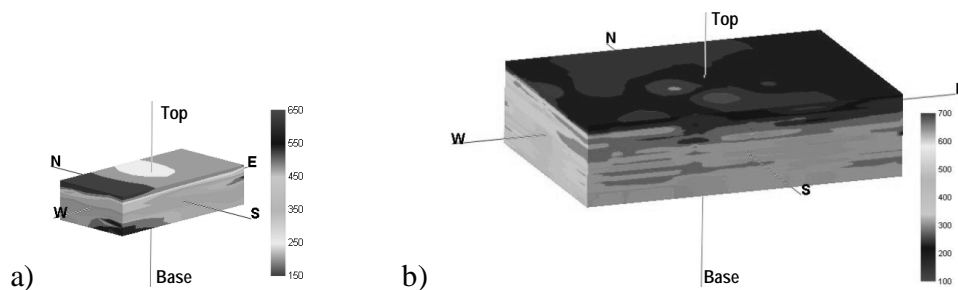


Fig. 2 Illustration of a 3D profile of the shear wave velocity, in m/s.

### 4.2 Vibration transmission through the ground

Fig. 3 shows the 2D FEM models used to assess the transmission of vibration from the Metro station to the building foundations and basement walls. In case a), the model covers a section of the ground 172.5 m wide and 44.0 m deep with 0.4 m square elements, i.e., the highest significant frequency lies in the range 100 – 150 Hz. In case b), the model covers a ground section 202.1 m wide and 40.9 m deep, again built with 0.4 m square elements.

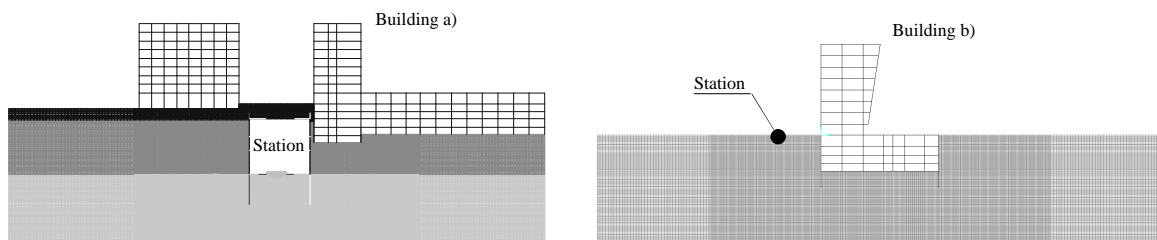


Fig. 3 2D FEM transversal model.

The transfer functions between the acceleration close to the rails and the acceleration in the building foundations and basement walls (Fig. 4) was calculated by step-by-step time integration for a pulse signal corresponding to a flat Fourier spectrum with amplitude equal to the unity. In case a), amplification is around 15 at 31.5 Hz and 4 at 70 Hz. The transfer functions are

significantly different for case b), where much less amplification occurs below 40 Hz, mainly due to the thicker backfill layer in case b).

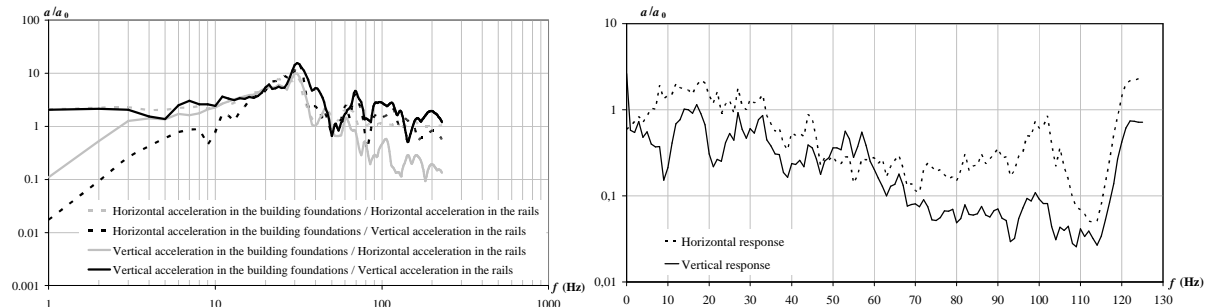


Fig. 4 Acceleration transfer functions from the Metro station to the building foundations and basement walls for cases: a) in the left-hand side; and b) in the right-hand side.

As measurements showed that the railway traffic induced vibrations were relevant only when trains were close to the station, there was no need to build a longitudinal 2D model.

## 5 CHARACTERISATION OF THE BUILDING

### 5.1 FEM models

Fig. 5 shows two of the several 3D FEM models used to assess the vertical transmission of vibration through the building structure. In case a), three different rooms were analysed in floors 1, 3 and 7, and a different model was built for each floor. Rooms 1, 2 and 3 (along the back wall of the building and not visible in Fig. 5) are the same for each floor and have a height of 2.80 m and a floor area of  $4.90 \times 3.50 \text{ m}^2$ ,  $3.90 \times 3.47 \text{ m}^2$  and  $4.50 \times 3.50 \text{ m}^2$ , respectively. The room walls were modelled with 15, 20 or 30 cm thick shell elements with a modulus of elasticity<sup>8</sup> ( $E$ ) of 6.65 GPa and a mass per unit volume ( $\rho$ ) around  $950 \text{ kg/m}^3$ . A constant damping ratio ( $\alpha$ ) of 8 % was assumed. In order to accurately assess the dynamic behaviour of the building for small amplitude vibrations, non-structural masonry walls were modelled with pin-jointed equivalent diagonal elements of width  $w_{eff} = 0.25d$ , where  $d$  is the length of the wall panel diagonal<sup>9</sup>. An elasticity modulus of 3.12 GPa was assumed for these diagonal elements which work on the wall plane only. In order to avoid unnecessary consideration of local vibration modes, the mass of these elements was distributed on the slabs and only the floors adjacent to the rooms considered in each case were modelled with shell elements. The other floors were modelled as diaphragms. An elasticity modulus of 30.5 GPa and a constant damping ratio of 5 % were assumed for all concrete floors, beams and columns. Modal analysis indicated the following global natural frequencies for case a):

- First mode (mainly along the  $x$ -axis including some torsion):  $f = 2.20 \text{ Hz}$ ;
- Second mode (mainly along the  $y$ -axis):  $f = 2.50 \text{ Hz}$ ;
- Third mode (mainly torsion):  $f = 3.89 \text{ Hz}$ .

In case b), as the area of walls is small (the building façade is mainly glazed), the diagonal elements were not considered. Considering open-spaces, the sound fields will be controlled by floor vibration at low frequencies. Predictions were obtained at floors 1, 2 and 7 using 20 cm

shell elements and a constant damping ratio ( $\alpha$ ) of 5 %. Modal analysis indicated the following global natural frequencies for case b):

- First, fourth and fifth modes (mainly along the  $y$ -axis):  $f_1 = 0.50$  Hz;  $f_4 = 1.91$  Hz;  $f_5 = 2.71$  Hz;
- Second and third modes (mainly along the  $x$ -axis):  $f_2 = 1.08$  Hz;  $f_3 = 1.52$  Hz;
- Sixth mode (mainly torsion):  $f_6 = 2.86$  Hz.

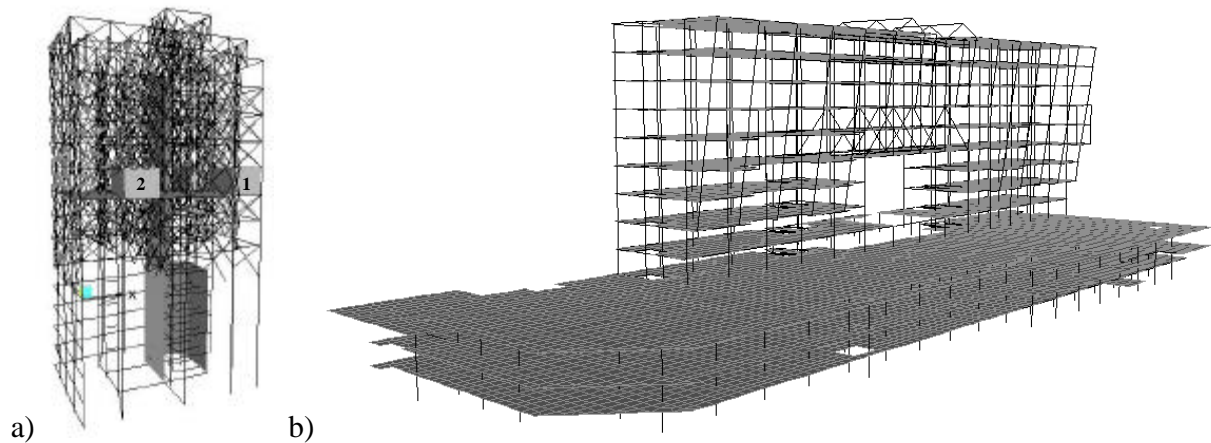


Fig. 5 3D FEM models used for assessing vibration in different rooms.

## 5.2 Vibration transmission through the building

Fig. 6 shows the envelopes of the acceleration transfer functions between the building foundations/basement walls and the walls and floors of the first floors of both cases.

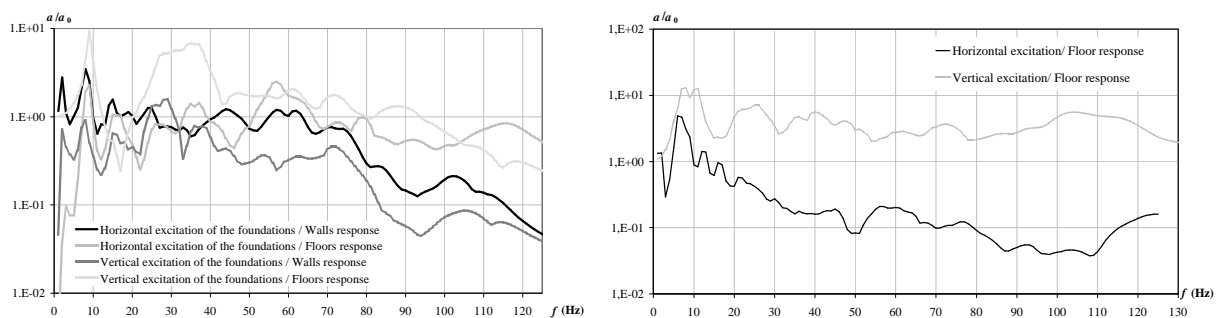


Fig. 6 Acceleration transfer functions from the building foundations to the walls and floors of the first floor of cases: a) in the left-hand side; and b) in the right-hand side.

Fig. 6 indicates that annoyance due to excessive vibration also is more likely to be caused by the floors than by the walls in case a). The significant amplification exhibited by the floors at 10 Hz and in the range 25 – 40 Hz could actually be reduced if a damping ratio varying from 15 % at 10 Hz to 5 % at 125 Hz were considered<sup>10, 11</sup>. However, considering the high energy content exhibited around 30 Hz by the acceleration spectra close to the rails (Fig. 1) and the significant amplification exhibited, at those same frequencies, by the acceleration transfer functions from the rails to the building foundations (Fig. 4) and then to the room floors and walls (Fig. 6), high levels of vibration are expected at the 31.5 Hz one-third octave band in case a). In

case b), significant amplification is observed around 10, 25, 40 and 100 Hz for vertical excitation. Again, as higher damping ratios can be expected, the obtained amplification is somewhat overestimated.

In order to check the room occupants tolerance to these vibration levels, an annoyance threshold was set according to the standard ISO 2631<sup>12</sup> and to reference values indicated by Nelson<sup>13</sup>. In Fig. 7, the comfort limit is compared with the envelopes of the one-third octave band acceleration level spectra obtained at the floor and ceiling of room 1 in the first floor of building a) for the three levels of rail excitation defined in Fig. 1. Although the room occupants are not likely to be annoyed by the lowest level of excitation, a slight increase of the excitation amplitude might be enough to induce significant annoyance at the 31.5 Hz one-third octave band. Fig. 7 also shows the average measured spectra of acceleration level. The shapes of the measured and predicted spectra are in good agreement, although predictions overestimate the vibration response.

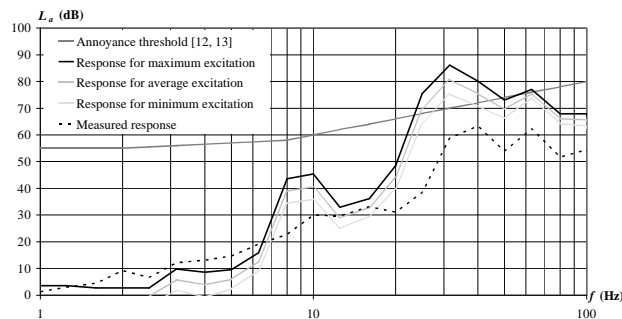


Fig. 7 Envelopes of the one-third octave band acceleration level spectra obtained at the floor and ceiling of room 1 in the first floor of building a).

In case b), the limits given in BS 6472<sup>14</sup> were considered to assess annoyance of occupants due to floor vibration. In spite of the significant amplification shown in Fig. 6, the absolute values of floor acceleration are not likely to cause annoyance, as shown in Fig. 8. Measurements of floor acceleration caused by railway traffic validated estimates. As floors in building b) correspond to thin flat slabs with larger spans than in building a), damping is probably less in building b) and thus the estimates are in better agreement with measurements.

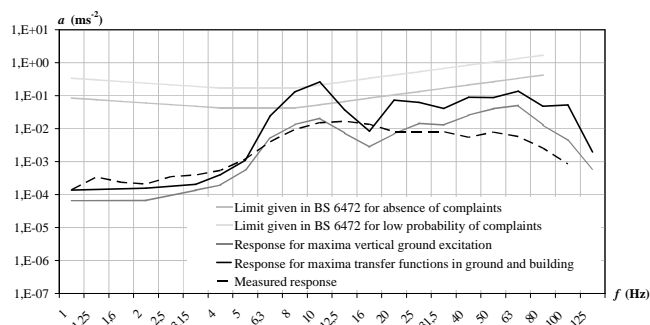


Fig. 8 Envelopes of the one-third octave band acceleration spectra obtained at the floor and ceiling in the first floor of building b).

### 5.3 sound transmission through the building

As the acoustic impedance of heavy walls and floors is much higher than that of the air, the numerically assessed vibration fields of walls and floors were used to calculate sound fields in the rooms by natural mode analysis. Using Kihlman's approach [15], the sound field generated in a room with dimensions  $a \times b \times c$  by a vibrating surface (wall, floor or ceiling) can be given by a Fourier expansion

$$p(x,y,z,t) = -j\omega r_0 \sum_{l,m,n=1}^{\infty} \frac{c_0^2 (-1)^l C_{mn} \mathbf{j}_{lmn}(x,y,z)}{L_{lmn} [(\omega_{lmn} + j\mathbf{d})^2 - \omega^2]} e^{j\omega t}, \quad (1)$$

where  $L_{lmn} = \int \mathbf{j}_{lmn}(x,y,z)^2 dV$ ;  $r_0$  ( $\text{kg/m}^3$ ) is the static value of air density; and  $\mathbf{d}$  describes the damping effect caused by sound absorption at the surface of walls and floors. As sound absorption in dwellings is negligible at low frequencies,  $\mathbf{d}$  lays around 1.5.

The functions describing the acoustic modes ( $l,m,n$ ) are given by

$$\mathbf{j}_{lmn}(x,y,z) = \cos\left(\frac{l\pi x}{a}\right) \cos\left(\frac{m\pi y}{b}\right) \cos\left(\frac{n\pi z}{c}\right), \quad (2)$$

and the corresponding eigenfrequencies by

$$\omega_{lmn} = c_0 \pi \sqrt{\left(\frac{l}{a}\right)^2 + \left(\frac{m}{b}\right)^2 + \left(\frac{n}{c}\right)^2}. \quad (3)$$

The factors  $C_{mn}$ , which describe the modal coupling between the vibrating wall or floor and the sound field in the room, are given by

$$C_{mn} = \int_0^b \int_0^c v_x(y,z) \cos\left(\frac{m\pi y}{b}\right) \cos\left(\frac{n\pi z}{c}\right) dy dz, \quad (4)$$

where  $v_x(y,z)$  is the function which describes, on the frequency domain, the velocity field of the construction element. As this velocity field is obtained from the FEM model for each node of the construction elements, the integral in eq. (4) has to be solved numerically.

As a consequence of the modal behaviour of sound fields in dwellings at low frequencies, eq. (1) does not have to be calculated for every coordinate ( $x,y,z$ ) but only for a lower corner position, where the largest number of acoustic modes are excited. The sound pressure spectra in that point can then be computed by adding the sound pressure generated by each vibrating wall or floor in the room.

In Fig. 9, the one-third octave band sound pressure level spectra obtained for room 1 in the first floor of building a) for the three considered levels of excitation are compared with comfort criteria given by Broner<sup>16</sup> and Inukai<sup>17</sup> and also with the normal equal-loudness-level contours for pure tones corresponding to the hearing threshold and to 30 phon<sup>18</sup>.

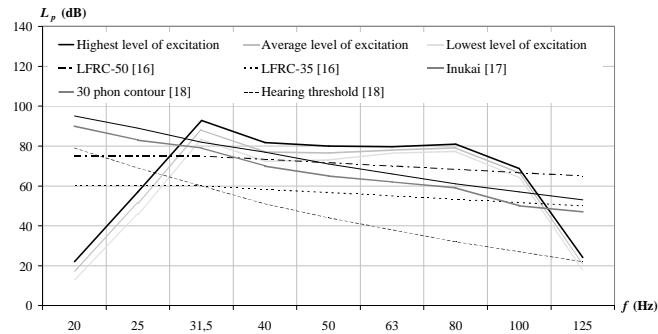


Fig. 9 One-third octave band sound pressure level spectra obtained for room 1 in the first floor of building a) and comfort criteria.

Fig. 9 shows that even for the lowest level of excitation, acting simultaneously at the three directions,  $x$ ,  $y$  and  $z$ , high sound levels appear in the range 31.5 - 80 Hz one-third octave bands. However, as these estimates were obtained from the overestimated vibration levels indicated in Fig. 7, annoyance due to low frequency noise does not occur. Measurements of sound pressure level confirmed this assumption.

In Fig. 10, the one-third octave band sound pressure level spectra obtained for the open-space in the first floor of building b) are compared with comfort criteria and with measurements.

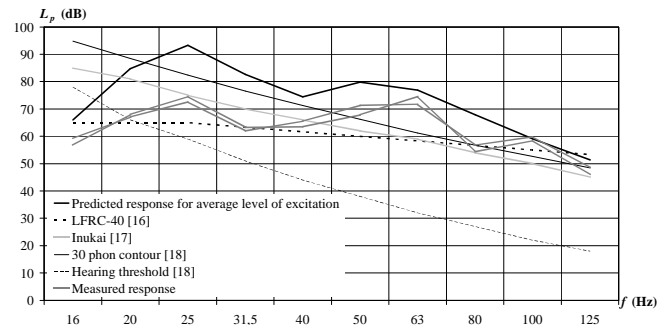


Fig. 10 One-third octave band sound pressure level spectra obtained for the open-space in the first floor of building b) and comfort criteria.

Fig. 10 shows that predictions of sound pressure level were overestimated below 50 Hz. Again, the shapes of predicted and measured spectra are in good agreement, which suggests that damping is controlling the accuracy of predictions.

## 6 SUMMARY AND CONCLUSIONS

In this paper, FEM and natural mode analysis were used to predict vibration and sound levels in buildings to be constructed near underground and surface railway stations. Measurements of vibration and sound levels made after construction of the buildings proved that the models are adequate for predictive assessment of annoyance due to low frequency noise, although they depend strongly on accurate estimates of damping. Thus, further studies are required in order to identify the main vibration transmission paths in buildings with concrete structures.

## 7 REFERENCES

1. M. Bahrekazemi, *Train-induced ground vibration and its prediction*, Ph.D. Thesis, Royal Inst. of Tech., Stockholm, Sweden, (2004).
2. K. Hayakawa, “Vibration protection in urban underground railways and its evaluation”, *Inter-Noise 94*, Yokohama, Japan, 145 – 148, (1994).
3. CSI - Computers and Structures, Inc., “SAP2000 User’s Manual”, Berkeley, California, USA, (2007).
4. F. Sécio, “Metropolitano de Lisboa: Red line expansion”, *Int. Seminar on Tunnels and Underground Works*, LNEC, Lisbon, Portugal, (2006).
5. RPS, “CROSSRAIL - Groundborne noise and vibration prediction – Validation on DLR Greenwich - Tech. Report 1E315-GOE00-00002”, London, UK, (2004).
6. TECNASOL-FGE, “Edifício de Escritórios do Sporting, Lisboa – Estudo Geológico-Geotécnico, Relatório para INVESCON – Investimentos e Construção, Lda.”, Lisbon, Portugal, (2001);
7. Y. Ohta, N. Goto, “Empirical Shear Wave Velocity Equations in Terms of Characteristic Soil Indexes”, *Earthquake Eng. & Str. Dynamics* 6, 167 – 187, (1978).
8. L. Godinho, *Propagação de ondas em sistemas que requerem o estudo da interação sólido-fluido*, Ph.D. Thesis, Univ. of Coimbra, Portugal, (2003).
9. M.J.N. Priestley, “Seismic design of masonry buildings – background to the draft masonry design code DZ 4210”, *Bulletin of the New Zealand Nat. Soc. for Earthquake Eng.* 13, (1980).
10. R. Craik, *Sound transmission through buildings using statistical energy analysis*, Gower, UK, (1996).
11. CEN, *EN 12354-1: Building acoustics – Estimation of acoustic performance of buildings from the performance of elements – Part 1: Airborne sound insulation between rooms*, Brussels, Belgium, (2000).
12. ISO, *ISO 2631 - Guide for evaluation of human exposure to whole-body vibration*, (1978).
13. P.M. Nelson, *Transportation noise reference book*, Butterworths, UK, (1987).
14. T. Kihlman, “Sound radiation into a rectangular room. Applications to airborne sound transmission in buildings”, *Acustica* 18 (11), 11 – 20, (1967).
16. N. Broner, “Low frequency sound quality and HVAC systems”, *Inter-Noise 94*, Yokohama, Japan, 1101 – 1104, (1994).
17. Y. Inukai *et al.*: “Unpleasantness and acceptable limits of low frequency sound”, *Journal of Low Freq. Noise, Vibration and Active Control* 19 (3), 135 – 140, (2000).
18. ISO, *ISO 226 – Acoustics: Normal equal-loudness-level contours*, (2003).